Journal of Power Sources 199 (2012) 331–335

Contents lists available at SciVerse ScienceDirect

Journal of Power Sources

journal homepage: www.elsevier.com/locate/jpowsour

Short communication

Natural cellulose as binder for lithium battery electrodes

S.S. Jeong*, N. Böckenfeld, A. Balducci, M. Winter, S. Passerini**

Westfälische Wilhelms Universität, Institut für Physikalische Chemie, Corrensstr. 28/30, 48149 Münster, Germany

ARTICLE INFO

Article history:
Received 28 July 2011
Received in revised form
16 September 2011
Accepted 29 September 2011
Available online 5 October 2011

Keywords:
Lithium-ion batteries
Natural cellulose
$LiFePO_4$
Graphite
Ionic liquid solvent
Phase inversion process

ABSTRACT

This manuscript reports on the development of lithium-ion battery electrodes based on natural cellulose as the binder. In particular, the cellulose binder is dissolved into fully recyclable ionic liquid to make volatile solvent-free slurries, which are coated on typical battery current collectors. Finally, the ionic liquid solvent is removed by a phase inversion process using water as the co-solvent. In such a way, electrodes can be prepared without using polluting volatile organic compounds. Full lithium-ion cells were made using graphite (SLP30) and carbon coated lithium iron phosphate ($LiFePO_4$, LFP) as active materials and 1 M $LiPF_6$ in EC-DEC (3:7 wt. ratio) based electrolyte. The lithium ion cells showed a stable specific capacity of 123 mAh per gram of $LiFePO_4$ at room temperature. This promising result shows that natural cellulose dissolved in a non-volatile ionic liquid can be used to manufacture battery electrodes thus providing new greener opportunities for the lithium-ion battery technology.

1. Introduction

Li-ion batteries are the most powerful electrochemical energy storage devices and for such a reason they are widely used in many portable electronic devices and considered as exceptionally promising candidates for the next generation of hybrid electric vehicles. However, the present Li-ion technology involves the use of rather polluting materials and industrial processes. For example, polyvinyliden-di-fluoride (PVdF), which is the most popular polymer used as binder in battery electrodes, requires the use of volatile and toxic solvents for processing, such as N-methyl-pyrrolidone (NMP). In addition, PVdF and NMP are expensive materials not so easy to recycle at end of the battery life. However, people are more and more concerned about eco-environmental issues. Improvements of good production, such as the development of low-energy, low-pollution production and recycling processes, and the use of green and/or natural materials, are very welcome.

Aqueous polymers are promising candidates as new binder or additive for lithium ion battery [1,2]. Recently, several works have reported their use as aqueous binder for but also to avoid the use of PVDF and its volatile and toxic solvent, NMP. In particular, sodiumcarboxymethylcellulose (NaCMC or CMC) was proposed to replace PVdF as the binder forlithium-richlayered oxides [3], graphite [4–7], silicon [8] and lithium iron phosphate ($LiFePO_4$, LFP) electrode [9–12]. CMC is a water-soluble derivative of cellulose. Its use in the battery technology allows a greener processing since the electrode slurry process does not requires the use of volatile and toxic organic solvents. Other advantages of CMC vs. PVdF are the lower cost and easy disposability at the end of life. Nevertheless, CMC is chemically derived from natural cellulose, and thus it still requires the need of chemical processes [13].

Natural cellulose, the most abundant renewable material, is intrinsically greener than any industrially synthesized polymer, such as PVdF. Cellulose, which has a wide application in human life, is obtained from wood and cotton as well as other plants. It can be used (and regenerated) as paper, paperboard, tissue paper, cellophane, rayon. Another important feature of natural cellulose is the lower cost, even with respect to CMC. The production cost of natural celluloses estimated at $0.5–$1.5 per kg depending on the yearly production.

Although cellulose can be considered the most environment-friendly binder, because it would not require any chemical processing beside the separation from vegetable sources, it is practically insoluble in any solvent and for that reason it is not easily processable. In the last few decades, however, ionic liquids (ILs), salts that are molten even at sub-ambient temperatures [14], have been developed which are capable of dissolving cellulose [15–17]. These materials have also been shown as very promising material for battery-related applications as, among many others, safer electrolytes and solvents for the synthesis of active electrode materials [11,12,17]. Their most important features are: low (or absent) volatility and flammability, wide liquidise temperature

* Corresponding author. Tel.: +49 251 8336024; fax: +49 251 8336084.
** Corresponding author. Tel.: +49 251 8336026; fax: +49 8336031.
E-mail addresses: sangsik.jeong@uni-muenster.de (S.S. Jeong), stefano.passerini@uni-muenster.de (S. Passerini).

0378-7753/$ – see front matter © 2011 Elsevier B.V. All rights reserved.
doi:10.1016/j.jpowsour.2011.09.102

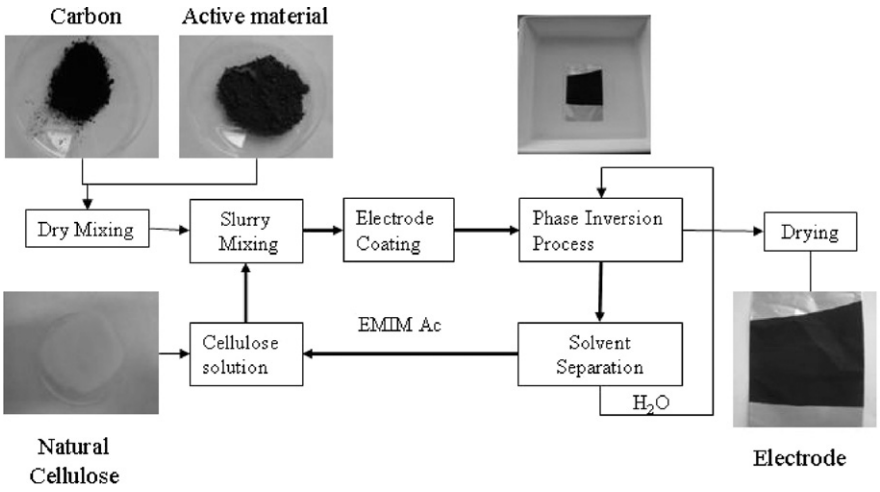

Fig. 1. Innovative production process for Li-ion battery electrodes. See text for further details.

range, and high thermal stability. For these characteristics ILs are very attractive solvents for green processing since their practically full recyclability (no vapour loss or decomposition during processing).

In this work, we report our investigations on the use of natural cellulose, dissolved in fully recyclable ionic liquids, as binder in lithium-ion battery technology. After coating the cellulose-based electrode slurries on appropriate substrates, the ionic liquid solvents are removed by phase inversion process using water (or natural alcohols) as co-solvent. As a result, electrodes can be manufactured without the need of polluting volatile organic compounds. Li-ion cells composed of $LiFePO_4$ and SLP30 as active materials have been realized using natural cellulose as the binder. The result showed in this paper clearly demonstrates the feasibility of using green-materials and green processing to produce Li-ion batteries.

2. Experimental

2.1. Electrode preparation

Commercial carbon-coated $LiFePO_4$ (LFP: Süd-Chemie, average particle size: 0.5 μm; carbon content: 2.3 wt.%) and SLP30 (TIMCAL, average particle size: 16 μm) were used as delivered. Natural cellulose was used as the binder for the both electrodes while Ketjen black (AKZO Nobel) and Super-P (TIMCAL) were used as conductive agents.

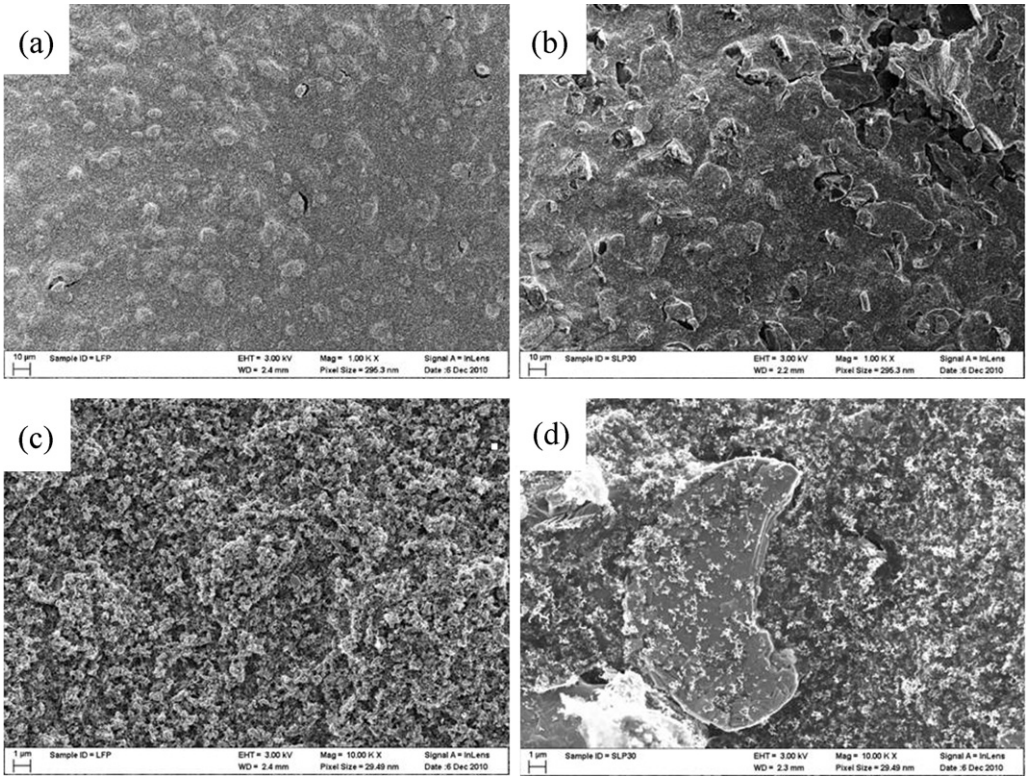

Fig. 2. SEM images of $LiFePO_4$ electrodes (a and c) and graphite electrodes (b and d) based on natural cellulose as binder.

The electrode making process is depicted in Fig. 1. The electrode active materials (LFP and SLP30) were, prior to slurry preparation, blended with the carbon additive (ketjen black and Super-P, respectively) for 30 min. 2 wt.% solution of natural cellulose (C6663 long fibers, Sigma–Aldrich) in 1-ethyl-3-methylimidazolium acetate (EMIMAc, BASF) was prepared at room temperature with the help of magnetic stirring. The dry mixtures of active material and the conductive carbon were dissolved into the cellulose solutions and homogenized by magnetic stirring for 12 h. LFP-containing slurries were cast on aluminum foils (20 μm, purity >99.9%) while SLP30-containing slurries were cast on Cu foil (20 μm, purity >99.9%) by using a laboratory doctor blade coater. The coated electrodes were immediately immersed in water to favor the phase inversion process and extract EMIMAc. Water, in fact, is a good solvent for EMIMAc but not for cellulose. The immersion of the slurry in water causes the dissolution of EMIMAc in the water phase and the consequent precipitation of cellulose resulting in the formation of a rigid matrix trapping the active material particles. After immersion in water for 30 min, the electrodes were dried in air for 2 h. EMIMAc was fully recovered (>99 wt.%) from the water solution by evaporation of the latter.

The coated electrodes were dried at 60 °C in a drying oven. Disk electrodes were cut with an area of 1.13 cm^2. The disk electrodes were dried at 120 °C under vacuum for 24 h to ensure the complete water removal [12]. The composition of the dried cathode electrode was 85.3 wt.% $LiFePO_4$, 10.7 wt.% Ketjen black and 4 wt.% of cellulose while that of the anode electrode was 90 wt.% SLP30, 5 wt.% Super-P and 5 wt.% of cellulose. The mass loading of the electrodes ranged between 2.5 and 4.1 mg cm^{-2}.

2.2. Cell assembly and characterization

The LFP and SLP30 electrodes were tested in Swagelok type cells assembled in an argon filled dry-box (H_2O <1 ppm, O_2 <1 ppm). Half-cells were realized by stacking an electrode disk, a polypropylene separator (Freudenberg, FS2190) drenched with the electrolyte (1 M $LiPF_6$ in EC:DEC (3:7 wt.)) and a Li disk (Chemetall, 0.05 mm). Analogously, Li-ion full cells were assembled using one LFP electrode as the cathode and one SLP30 electrode as the anode. All cells were equipped with a lithium metal quasi-reference electrode.

The cells were tested using the typical constant current (CC)-constant voltage (CV) test protocol cycle performances were carried out with constant current charge/discharge (CC step) at 20 °C ± 2 °C using a Basytec Battery tester. The voltages quoted in this manuscript are always referred to that of lithium.

3. Results and discussion

Fig. 2 shows the SEM images of the LFP (a and c) and SLP30 (b and d) electrodes prepared by using natural cellulose as binder. The SEM image reported in Fig. 2a, shows the existence of globular aggregation in the LFP electrode, which have a dimension of several micrometers. These globular particles consist of LFP, carbon and binder as shown by the high magnification SEM image (Fig. 2c). On the other hand, no aggregation is observed in the anode electrode (Fig. 2b) because of the already large dimension (about 15 μm; see Fig. 2d) of the SLP30 particles. The high magnification SEM images in Fig. 2(c and d) of LFP and SLP electrodes show as a network of Super P and cellulose is surrounding the active material particles.

Fig. 3 shows the room temperature cycle performance of LFP electrode between the 2.8 V and 4.2 V voltage limits, in half-cell configuration. As shown in Fig. 3a, changes in the cell capacity and voltage plateau are observed at different charge/discharge current rates. The LFP electrode was able to deliver a specific capacity of

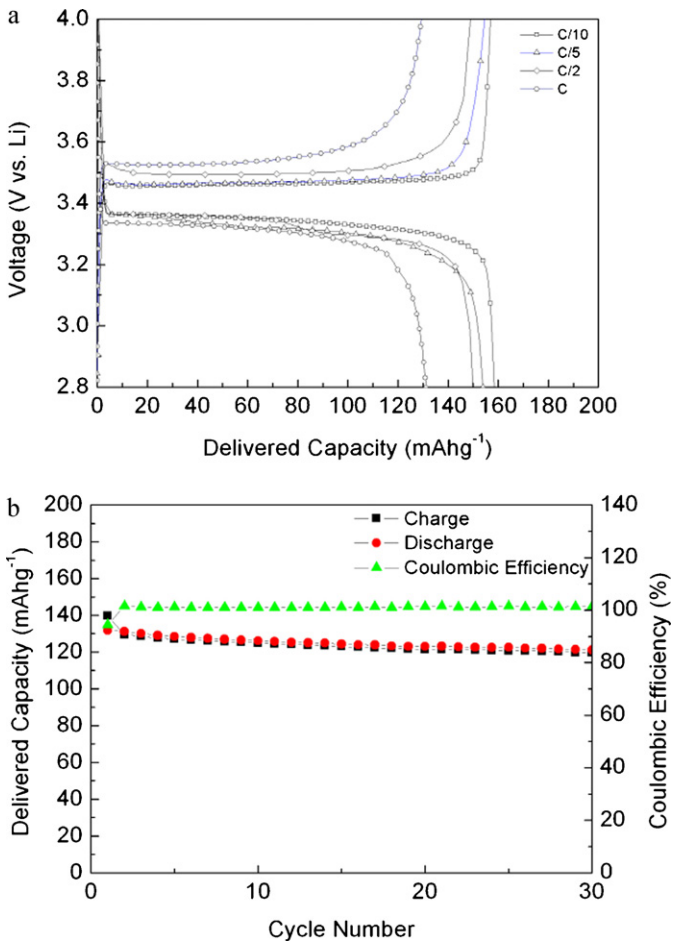

Fig. 3. Voltage profile vs. capacity at different C rates (a) and cycle performance at 1 C rate (b) of LFP electrodes based on cellulose binder. The tests were performed at room temperature. See further details in Section 2. The anomalous average cycle efficiency of 101% is due to the instrument accuracy (±0.5% full I scale) in integrating the current.

160 mAh g^{-1} in the test performed at C/10 charge and discharge rates. The discharge voltage plateau of the LFP electrode is observed at about 3.35 V. The specific capacity of the LFP electrode slightly decreased to 155 mAh g^{-1} at C/5 and 150 mAh g^{-1} at C/2. However, only a capacity of 130 mAh g^{-1} was delivered by the electrode at 1 C. During the following long-term cycling at 1 C rate (see Fig. 3b) the delivered capacity slightly decreases to 125 mAh g^{-1} in the initial few cycles. However, the electrode showed excellent capacity retention of 92% after 50 cycles (Fig. 3b).

The discharge curves in Fig. 3a also shows as the discharge voltage plateau of the LFP electrode is not strongly affected by the rate change from C/10 to 1 C. In general, the composite electrode capacity decreases upon increasing C rates because of higher ohmic drop (low electronic conductivity) and/or limited Li^+ ion diffusion in the electrolyte filling the electrode pores [18]. The slight decrease of the LFP electrode voltage plateau on increasing rates indicates that the electronic conductivity of the composite electrode is certainly not the cause for the decreased performance. Thus, the capacity decrease is to be associated with a limited Li^+ ion supply to (or drain from) the LFP particle/pore electrolyte interface. This could be due to the existence of the globular aggregates in the LFP electrodes (see SEM images Fig. 2), which internal porosity might not be completely filled by the electrolyte. Optimization of the LFP electrode morphology is certainly needed; nevertheless, the electrode performance in terms of delivered capacity and cyclability is rather promising considering the novelty of the process used. The binding

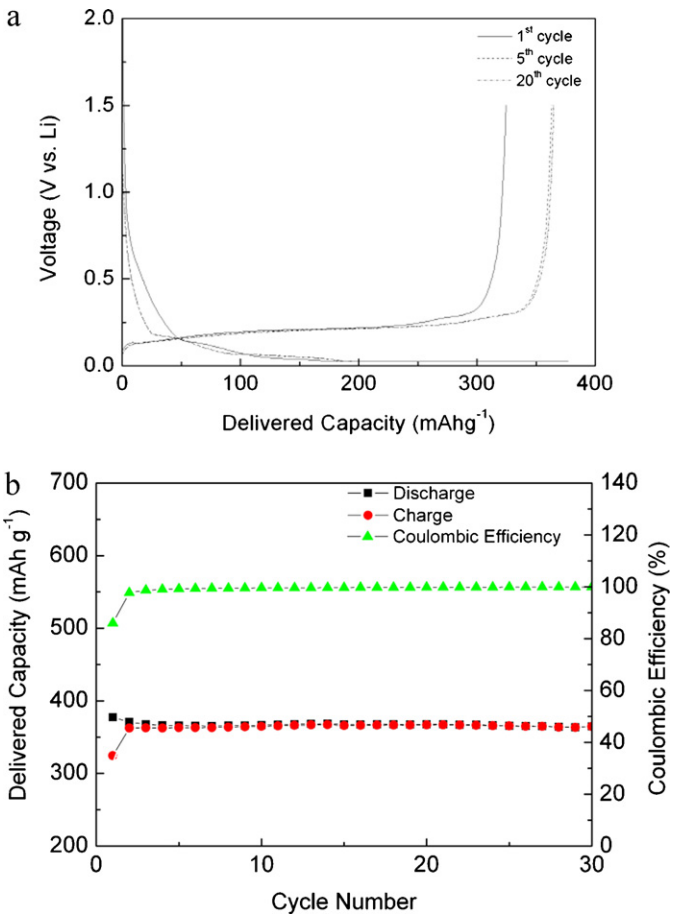

Fig. 4. Voltage profile vs. capacity (a) and cycle performance (b) of a SLP electrode based on cellulose binder. The tests were performed at room temperature and 1 C charge/discharge rate. See further details in Section 2. The anomalous average cycle efficiency of 101% is due to the instrument accuracy (±0.5% full I scale) in integrating the current.

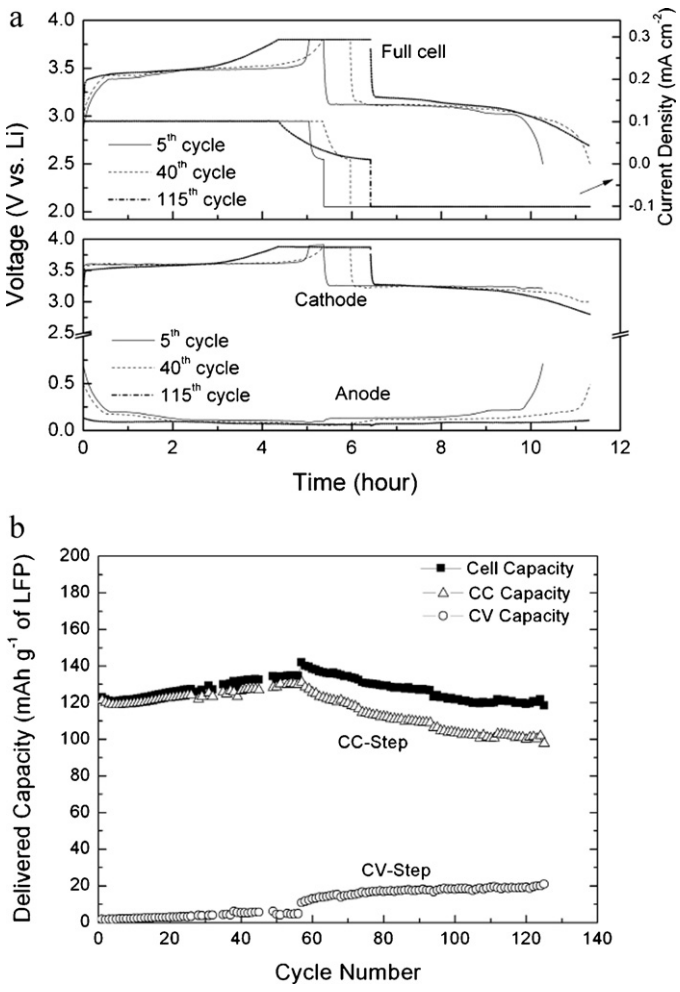

Fig. 5. Cell, cathode and anode voltage profiles recorded in different cycles (a) and cycle performance (b) of a full Li-ion cell employing cellulose-based LFP and SLP30 electrodes. The tests were performed at room temperature and C/5 charge/discharge rate. Active material cathode loading: 4.1 mg/0.71 mAh. Active material anode loading: 2.7 mg/1.0 mAh. See further details in Section 2.

capability of natural cellulose is certainly outperforming that of commonly used binders in the Li-ion technology, since it withstands the phase inversion process performed in water [19].

Fig. 4 shows the cycle performance of SLP30 electrodes tested in the voltage range extending from 1.5 V and 0.024 V at room temperature. These electrodes showed the theoretical specific capacity (370 mAh g^{-1}) at charge/discharge rates from C/10 to 1 C. For such a reason, only the results obtained at the highest rate (1 C) are shown. In Fig. 4a, are reported the voltage vs. capacity curves of the SLP electrode during the 1st, 5th and 20th charge/discharge cycles. In the figure it is easily observed, as the charge and discharge curves recorded at the 5th and 20th cycles are practically indistinguishable, which supports for a good cycling performance of the SLP electrode. Both the charge and discharge curves showed the typical behavior of graphite intercalation compounds [4–7,20].

The 1st cycle discharge curve evidences an increased capacity in the voltage region extending from 0.8 V to 0.2 V, which is typical of the irreversible solid electrolyte interphase (SEI) formation on graphite electrodes [21–23]. The SEI is formed at the expenses of the lithium insertion process and, as matter of fact, the amount of lithium extracted during the following step is lower than expected. The Coulombic efficiency at the 1st, 2nd, and 3rd cycles was 86, 97.7 and 98.7%, respectively. The cell showed a capacity retention higher than 98% after 30 cycles (see Fig. 4b).

Fig. 5 shows the room temperature cycling performance of a full Li-ion cell made using the cellulose-based electrodes. The cell was tested at C/5 rate, however, a CV step was inserted after the CC charge step to favor the graphite lithiation. The CV step was terminated when the current was lower than C/50. To avoid lithium metal plating on the graphite anode, the electrode mass loadings were properly balanced to make cathode-limited (LFP) cells. The cell capacity and the C rate were calculated by subtracting 20% of the anode capacity to the LFP electrode capacity to take into account the amount of capacity lost during the SEI formation.

In Fig. 5a is shown the cell, cathode and anode voltages during the 5th and 40th cycle. The applied current density is also reported to evidence the extension of the CV step. The comparison of the curves at the 5th and 40th cycles shows some peculiar differences. During the 5th cycle the cell capacity is clearly limited by the anode as indicated by the increase of the anode voltage at the 5th cycle. This is, somehow, in contrast with the nominal electrode capacities (LFP: 0.84 mAh; SLP30: 1 mAh) and the electrode rate performance results (see Figs. 3 and 4). However, the cell capacity appears to be limited by both electrodes at the 40th cycle as indicated by the voltage change of both electrodes at the end of the discharge cycle.

The increasing capacity of the graphite electrode, and, thus, of the entire cell, upon cycling is even more evident in Fig. 5b where the cell delivered capacity and the charge capacity taken by the cell during the CC and the CV steps are illustrated. The cell

capacity is observed to increase from the initial 120 mAh g^{-1}(LFP) to about 135 mAh g^{-1}(LFP) at the 50th cycle. This is clearly due to the increase of the charge during the CV step while the CC step charge does not substantially change. After a resting period of several days (55th cycle) the cell capacity increased further to more than 140 mAh g^{-1}(LFP). On further cycling, however, the cell capacity decreased to the initial value. This trend is frequently observed upon long-term cycle testing of swagelok-type cells. Visual inspection of these cells at the end of life reveals a scarcity of electrolyte in the separator and the electrodes, which is due to the fact that the empty volume in the cell is much higher than the electrolyte volume. The electrolyte loss in the active part of the cell results in the cell resistance increase as indicated by the continuous increase of the charge in the CV step during cycling. Nevertheless, after more than 120 cycles, the cell was able to deliver the same capacity as in the first cycle and more than 85% of the maximum capacity, as detected in the 57th cycle.

4. Conclusions

In this study, a new process to produce Li-ion battery electrodes was developed. The process can be considered green because it makes use of a natural, renewable material (cellulose), an easily recyclable ionic liquid (EMIMAc) and water.

The LFP and SLP30 composite electrodes made using natural cellulose as the binder displayed performance comparable to that of electrodes made using conventional binders. LFP/SLP30 full Li-ion cells displayed good capacity and cycling performance even in laboratory cells.

These promising results open up the way for the development of green, low cost processes in Li-ion battery technology.

Acknowledgments

The authors wish to thank the financial support of Evonik, Chemetall and Volkswagen within the framework of the sponsored "Applied Material Science for Energy Storage and Conversion" Chair at the University of Muenster.

References

[1] J. Drofenik, M. Gaberscek, R. Dominko, M. Bele, S. Pejovnik, J. Power Sources 94 (2001) 97–101.
[2] G. Nagasubramanian, D. Doughty, J. Power Sources 96 (2001) 29–32.
[3] J. Li, R. Klopsch, S. Nowak, M. Kunze, M. Winter, S. Passerini, J. Power Sources 196 (2011) 7687–7691.
[4] J. Drofenik, M. Gaberscek, R. Dominko, F.W. Poulsen, M. Mogensen, S. Pejovnik, J. Jamnik, Electrochim. Acta 48 (2003) 883–889.
[5] S.F. Lux, M. Schmuck, G.B. Appetecchi, S. Passerini, M. Winter, A. Balducci, J. Power Sources 192 (2009) 606–611.
[6] S.F. Lux, M. Schmuck, S. Jeong, S. Passerini, M. Winter, A. Balducci, Int. J. Energy Res. 34 (2010) 97–106.
[7] S. Pejovnik, R. Dominko, M. Bele, M. Gaberscek, J. Jamnik, J. Power Sources 184 (2008) 593–597.
[8] V.L. Chevrier, J.R. Dahn, J. Electrochem. Soc. 157 (2010) A392–A398.
[9] J.-H. Lee, J.-S. Kim, Y.C. Kim, D.S. Zang, U. Paik, Ultramicriscopy 108 (2008) 1256–1259.
[10] W. Porcher, B. Lestriez, S. Jouanneau, D. Guyomard, J. Electrochem. Soc. 156 (2009) A133–A144.
[11] S.F. Lux, S.-S. Jeong, G.-T. Kim, S. Passerini, M. Winter, A. Balducci, ECS Trans. 25 (2010) 21–25.
[12] G.T. Kim, S.S. Jeong, M. Joost, E. Rocca, M. Winter, S. Passerini, A. Balducci, J. Power Sources 196 (2011) 2187–2194.
[13] M.P. Adinugraha, D.W. Marseno, Haryadi, Carbohydr. Polym. 62 (2005) 164–169.
[14] G.B. Appetecchi, M. Montanino, M. Carewska, M. Moreno, F. Alessandrini, S. Passerini, Electrochim. Acta 56 (2011) 1300–1307.
[15] D.M. Phillips, L.F. Drummy, D.G. Conrady, D.M. Fox, R.R. Naik, M.O. Stone, P.C. Trulove, H.C. De Long, R.A. Mantz, J. Am. Chem. Soc. 126 (2004) 14350–14351.
[16] R.P. Swatloski, S.K. Spear, J.D. Holbrey, R.D. Rogers, J. Am. Chem. Soc. 124 (2002) 4974–4975.
[17] N. Recham, M. Armand, J.-M. Tarascon, C.R. Chim. 13 (2010) 106–116.
[18] G.T.-K. Fey, Y.G. Chen, H.-M. Kao, J. Power Sources 189 (2009) 169–178.
[19] S.S. Rahatekar, A. Rasheed, R. Jain, M. Zammarano, K.K. Koziol, A.H. Windle, J.W. Gilman, S. Kumar, Polymer 50 (2009) 4577–4583.
[20] S.R. Sivakkumar, J.Y. Nerkar, A.G. Pandolfo, Electrochim. Acta 55 (2010) 3330–3335.
[21] E. Peled, J. Electrochem. Soc. 126 (1979) 2047–2051.
[22] M. Winter, J.O. Besenhard, M.E. Spahr, P. Novák, Adv. Mater. 10 (1998) 725–763.
[23] H. Buqa, A. Wursig, J. Vetter, M.E. Spahr, F. Krumeich, P. Novak, J. Power Sources 153 (2006) 385–390.